

Oscillating-grid turbulence including effects of rotation

By STUART C. DICKINSON† AND ROBERT R. LONG

Department of Earth and Planetary Sciences, The Johns Hopkins University,
Baltimore, Maryland 21218

(Received 25 November 1980 and in revised form 9 July 1982)

Experiments were performed to investigate some aspects of turbulence in rotating and non-rotating fluid systems where the turbulence was induced by a horizontal grid oscillating vertically. An earlier theory by the second author made use of a planar source of energy, which appeared to be similar to the energy source of the grid, in determining the characteristics of the turbulence at points some distance away. The simplicity of the theory was in the parameterization of the grid ‘action’ by a single quantity K , with dimensions and characteristics of eddy viscosity.

The experimental results provide additional confirmation of the theory in the non-rotating case, and indicate the usefulness of the idealized energy source in the rotating case. In the latter, we measured the propagation of the front separating disturbed and undisturbed fluid, moving along the axis of rotation. The thickness $d(t)$ of the disturbed region increases at first as $(Kt)^{\frac{1}{2}}$, as in a non-rotating fluid, until the Rossby number $K/\Omega d_k^2$ becomes of order unity.

Beyond this the disturbances are wavelike and rotationally dominated, and the thickness now increases linearly with time, yielding a speed of propagation for the front proportional to the wave speed $(K\Omega)^{\frac{1}{2}}$. Finally, the disturbances reach the bottom and the vessel is in statistical steady state. Then a region of thickness d_k independent of time is found, and it contains motion that resembles ordinary, three-dimensional turbulence. $d_k \sim (K/\Omega)^{\frac{1}{2}}$ is analogous to the depth of the turbulent Ekman layer $H \sim (K/\Omega)^{\frac{1}{2}}$, where K is taken as an eddy viscosity.

McEwan constructed a similar rotating experiment, although with a different energy source, and observed vortices parallel to the axis of rotation, provided that the Rossby number was less than a critical value. Our observations and theory indicate that the disappearance of the vortices corresponds to $h < d_k$, where h is the total depth of the fluid. At that point, the whole tank is filled with three-dimensional turbulence.

1. Introduction

In 1955 Rouse & Dodu published a pioneering experimental paper in which a horizontal grid oscillating vertically created turbulence in a container of stratified fluid. Since then, many investigators have run similar experiments to determine the rate of erosion of a density interface (Cromwell 1960; Turner & Kraus 1967; Turner 1968; Brush 1979; Linden 1971, 1973; Wolanski 1972; Crapper & Linden 1974; Wolanski & Brush 1975; McDougall 1979; Folse, Cox & Schexnayder 1981) and to investigate the fundamental nature and spatial decay of the turbulence created by

† Present address: David W. Taylor Naval Ship Research and Development Center, Bethesda, Maryland 20084.

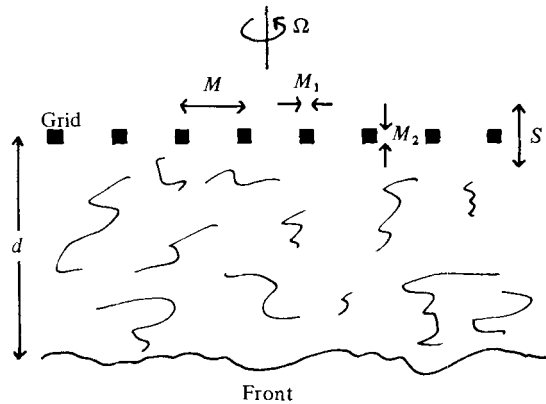


FIGURE 1. Schematic picture of oscillating-grid turbulence showing physical parameters. M , M_1 , M_2 are the dimensions and S is the stroke of the grid. Ω is the rotation rate of the container and d is the distance of the front from the grid.

the grid (Bouvard & Dumas 1967; Thompson 1969; Thompson & Turner 1975; Hopfinger & Toly 1976; Dickinson & Long 1978; McDougall 1979). Such turbulence is without mean flow or mean shear, and decays with distance from the grid in a way similar to the decay behind a grid in a wind tunnel. One of us (Long 1978*a*) recently proposed a theory to explain some of the features of this turbulence. The theory shows that a single quantity K (called 'action'), of dimensions and character of eddy viscosity, characterizes the oscillating grid (or other similar planar energy source).

A companion paper (Dickinson & Long 1978) applied the theory to a time-dependent problem of a grid suddenly started up in a resting fluid at time $t = 0$. A turbulent layer is created and grows in thickness (figure 1) as the front separating the disturbed and undisturbed fluid moves away. Its distance (d) from the grid is predicted by dimensional analysis to be

$$d = (Kt)^{\frac{1}{2}} F\left(\frac{K}{\nu}\right), \quad (1)$$

or, at high Reynolds numbers K/ν ,

$$d = (Kt)^{\frac{1}{2}}, \quad (2)$$

where we absorb the coefficient of proportionality in K . The first experiments of Dickinson & Long seemed to confirm this $t^{\frac{1}{2}}$ time-dependent behaviour, and showed how K could be determined as a function of the frequency of oscillation f , the stroke S and lengths M_1 , $M_2 \dots$ characterizing the oscillating grid by measuring d^2/t in (2).

Another paper (Long 1978*b*) extended the theory of the planar energy source to homogeneous decaying turbulence and to turbulence downstream of a grid in a wind tunnel. That paper suggested the fundamental character of this sample turbulence and the need for further experimentation. The present work was undertaken to increase our understanding of grid turbulence in simple cases and to extend its application to another system of geophysical interest – namely to a homogeneous rotating system. The use of a grid to produce the turbulence suggests that our interests are rather different from most experimental studies of turbulence in rotating systems (e.g. Küchemann 1965; Bretherton & Turner 1968; Strittmatter, Illingworth & Freeman 1970; Ibbettson & Tritton 1975).

After experimental work began, we discovered a paper by McEwan (1976), who had constructed a similar experiment in a rotating fluid. Instead of an oscillating grid, he used a system of jets into the vessel at the bottom as a planar energy source.

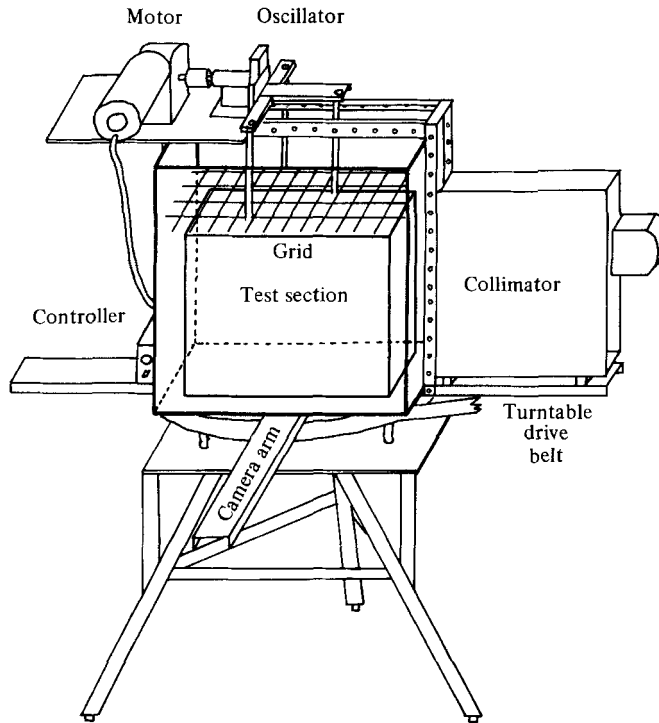


FIGURE 2. Diagram of the oscillating-grid apparatus and the rotating table.

McEwan's interests, although of great relevance to meteorology, were different from ours, and our observations in the rotating problem complement his.

2. Description of the experiment

Most of the experiments discussed in this paper were performed in a transparent Plexiglas tank, with rectangular shape $57 \times 57 \times 61$ cm (figure 2), chosen for optical reasons. The top was open to allow a free surface. Inside was an inner tank, $38 \times 38 \times 45$ cm, also open at the top, and glued to the bottom of the outer tank. This was introduced to reduce the 'mean' large-scale circulations (first mentioned by Cromwell 1960), which arise probably because of alignment and other difficulties, and which overturn large portions of the tank contents instead of producing an identifiable moving front.

The turbulence-generating equipment consisted of a grid, a support system, an oscillator transmission, and a controlled variable-speed motor. The grid elements were 0.95 cm square bars, notched and glued together with a solidity of 36% – the same as the grid of Rouse & Dodu – compared with 80% for the perforated plate of Bouvard & Dumas. The oscillation frequency f was varied from 1.0 to 2.5 Hz, but the amplitude (stroke S) was always 5 cm. The whole apparatus was on a rotating table to allow the experiments to be performed in either a rotating or non-rotating fluid system, at rotation rates up to 1.1 rad/s.

All direct measurements in these experiments were made photographically; therefore flow visualization had to be a prime consideration in the design of the equipment. Positively or negatively buoyant dyes, markers or particles could not be used unless their terminal buoyant velocity was much less than the turbulent velocity. This ruled out the use of hydrogen bubbles and many other markers.

The visualization scheme used for the bulk of the experiments was a suspension of aluminium flakes. These align with the local shear, and, when turbulence disturbs them, light and dark patches appear, marking the larger eddies. Good results were obtained using a slit of light from a collimator at 90° from the viewing angle for illumination. The collimator contained a water-cell infrared filter (to prevent convection in the tank), and it produced a slit of light 1 cm thick passing through the centre of the tank, parallel to the film plane of the camera. The steady-state turbulent layer was also identified by the diffusion of dye. Introduced at the grid, the dye would diffuse, eventually reaching uniform density in the turbulent layer. This was photographed against a white translucent sheet illuminated by a spotlight.

The cameras were mounted on the end of the long arm of the rotating table. In the pictures, the grid was at the top, and the bottom was about 45 cm below. A stainless-steel rod in the centre of the tank with markings every 10 cm served as a reference for distance from the midpoint of the grid stroke.

The rotation rate was measured by a microswitch relay and timer apparatus with maximum error of 0.1%. Fluctuations in rotation rate were not measured, but observation of the spinning tank and the sound of the motor both indicated that such fluctuations were not a significant source of error. Measurement of the grid-oscillation frequency was made to the nearest 0.1 Hz or a maximum error of 5% at 1 Hz.

Systematic errors due to optical distortion appeared to be small. The wide-angle lens used with the ciné camera had no apparent barrel distortion. The distortion due to the refraction of the light rays at the tank walls and to parallax was corrected by putting the ruled rod mentioned above in the plane of the measurements to give distance in the vertical direction. Since only vertical distances are involved in the measured phenomena, the small horizontal distortion did not affect the results.

The greatest source of error in these experiments was the measurement of the position of the interface, or the thickness of the layer of turbulence. Average positions were determined by eye, and the resulting accuracy is estimated to be ± 2 cm. A large number of measurements was made to reduce random errors. Most of the films were read by the first author, so that a systematic bias might exist. However, some measurements from the same films were made by others, and differences between observers were usually less than 1 cm. All in all, we believe that the scatter of the data presented in §3 should demonstrate the accuracy of these experiments.

3. Motion of the turbulent front in the non-rotating case

The average distance d of the front from the grid, and the time t at which the grid was started were recorded by still photographs and ciné films. The data for the square tank of the present experiments were analysed in much the same way as in the cylindrical tank of Dickinson & Long (1978). Each parameter set included at least five individual runs. They were plotted as d versus t on a log-log scale, but, instead of fitting a line by eye, a regression analysis was made using

$$d = K^{\frac{1}{2}} t^n, \quad (3)$$

or
$$\ln d = n \ln t + \ln K^{\frac{1}{2}} \quad (4)$$

and solving. The results of the regression are found in table 1 and in figures 3–5. The value of n in (3) was very close to 0.5, as the theory would suggest. This behaviour is the same as that discussed by Dickinson & Long (1978); but with our present larger equipment we found no deviation from the theoretical curve at large d , where sidewall effects seemed to influence the growth in the cylindrical vessel.

f	n	K^2	K	r^2
1.55	0.48	4.12	17.0	0.97
2.0	0.48	4.66	21.7	0.96
2.5	0.50	5.16	26.6	0.95

TABLE 1. Values of K and exponent n from the linear regressions of the oscillating grid in the non-rotating case. r^2 is the coefficient of determination.

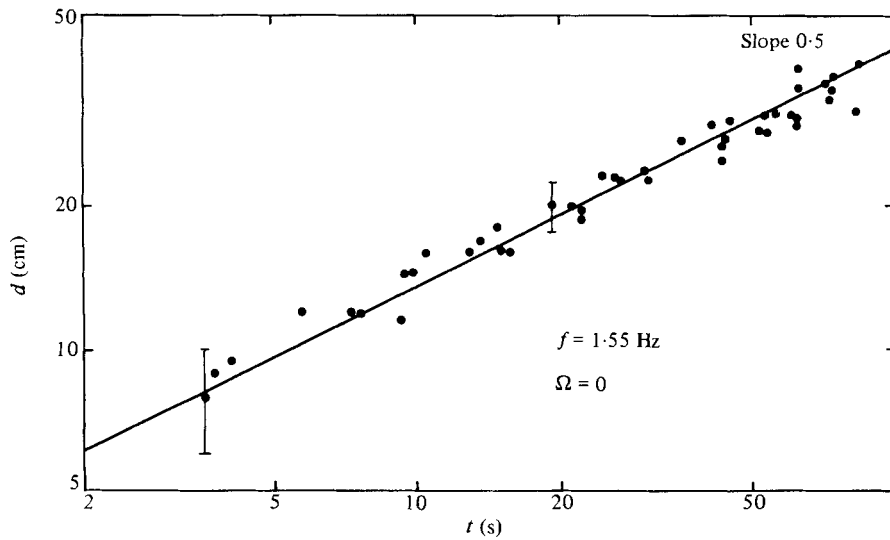


FIGURE 3. Graph of d versus t , non-rotating case; $K = 17.0$.

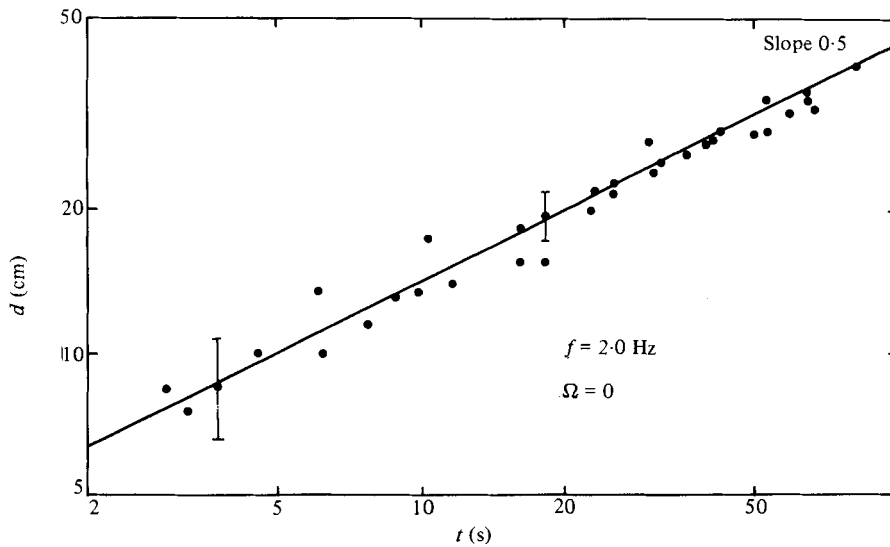


FIGURE 4. Graph of d versus t , non-rotating case; $K = 21.7$.

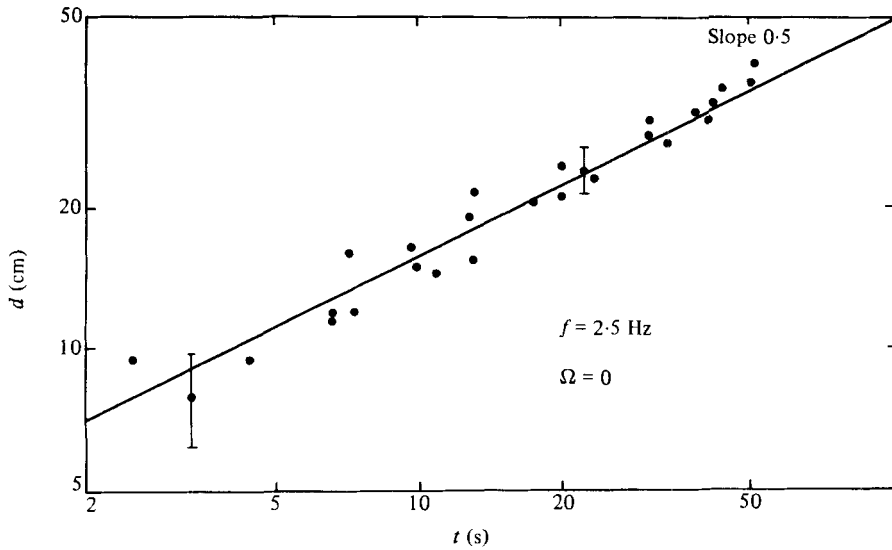


FIGURE 5. Graph of d versus t , non-rotating case; $K = 26.6$.

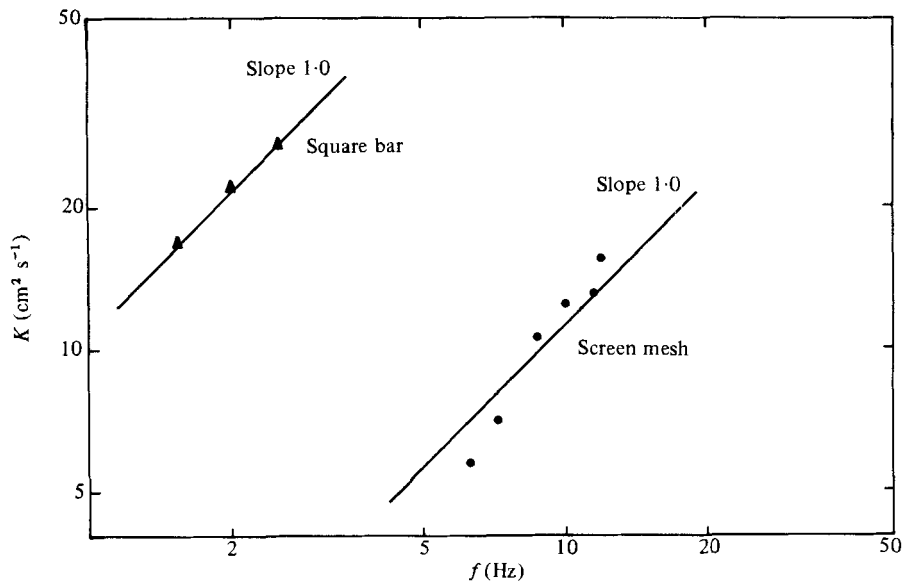


FIGURE 6. Values of action K for square bar and for circular screen mesh (from Dickinson & Long 1978) as function of frequency f .

One can also find the dependence of action K on the grid frequency for the two types of grids. The graphs of K versus f can be found in figure 6. The square-bar data are well fitted by a linear relationship in agreement with recent measurements by Folse *et al.* (1981). This is to be expected on dimensional grounds if viscosity is neglected. Comparing K with the physical grid parameters of action $K_g = fS^2$, we find $K = 0.43K_g$, $\Omega = 0$. However, earlier measurements in a cylindrical tank using a screen-mesh grid (Dickinson & Long 1978; Dickinson 1980) also shown in figure 6 suggested $K \propto f^n$, where n seemed larger than 1. Further experimentation is needed to determine whether this is a viscous effect.

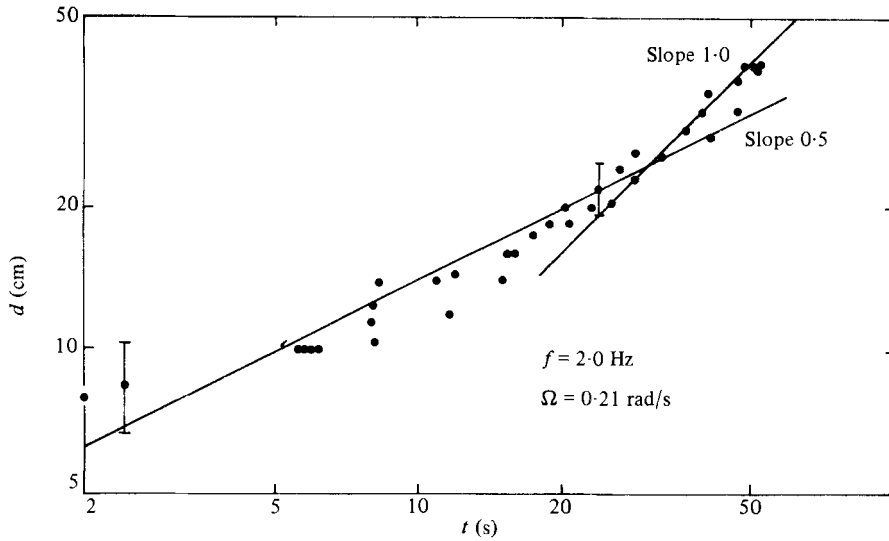


FIGURE 7. Graph of d versus t , rotating case; $K_g = 50$.

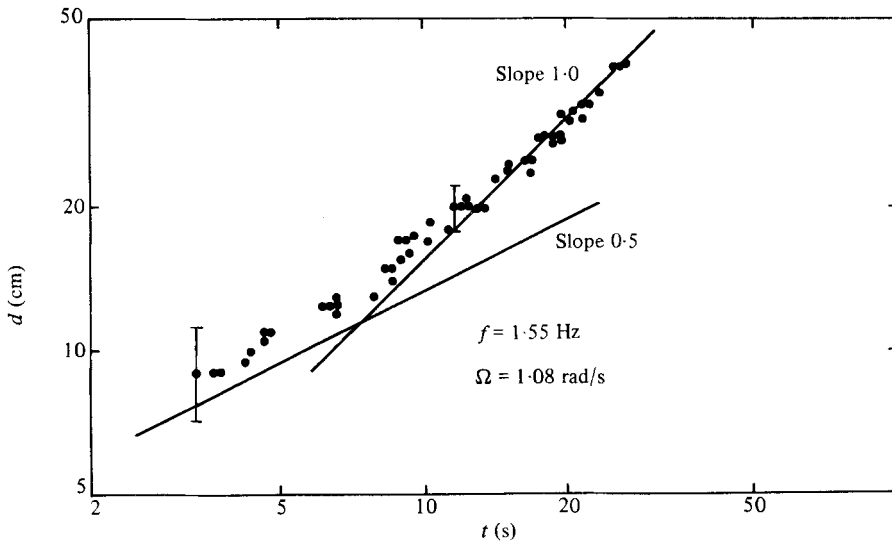


FIGURE 8. Graph of d versus t , rotating case; $K_g = 38.8$.

4. Motion of the turbulent front in the rotating case

In this case, the values of d and t were recorded from the ciné films and plotted logarithmically for each parameter set (f , Ω), as in figures 7–9. Each set is an ensemble of at least five independent runs.

We should expect the strong turbulence near the grid to be relatively unaffected by the rotation and, therefore, to be similar to the case of zero rotation. As a consequence, figures 7–9 contain lines of 0.5 slope taken from the corresponding case of $\Omega = 0$. The data at small t fit this slope well, but, as the front progresses, the slope increases and appears to follow a slope of 1.0, indicating that the front velocity approaches a constant. The lines of best fit were obtained by regression. The data

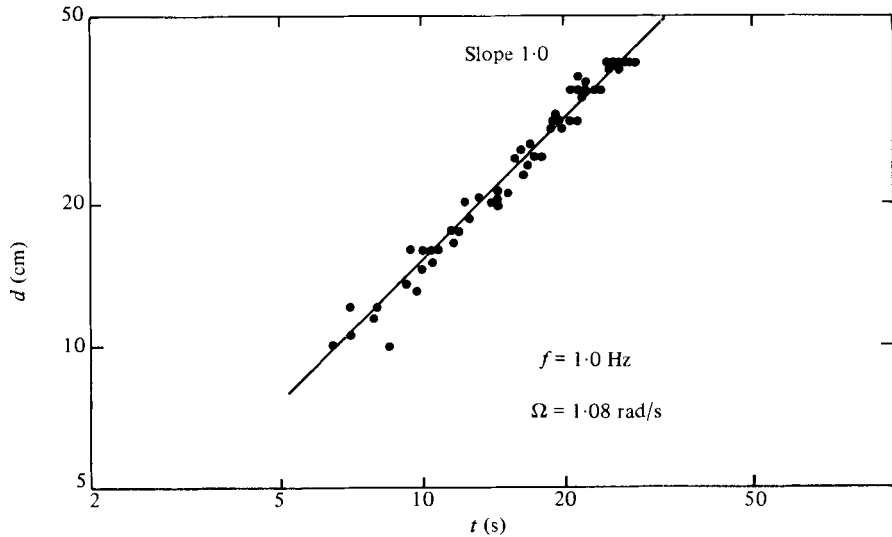


FIGURE 9. Graph of d versus t , rotating case; $K_g = 25$.

were analysed by regression, however, only for values of d and t for which a power law appears to exist, so that the data in the transition zone between power laws were not included in the regressions. The points included are a subjective judgment on the authors' part; however, the same criteria for inclusion were applied to each parameter set, so we feel comparisons can be made between sets. For the 0.5-slope region, the data were fitted to $d = K^{\frac{1}{2}}t^n$ as before. However, for the steeper-slope region, $d = K_{\Omega}^{\frac{1}{2}}t^n$ was used, where K_{Ω} is the coefficient for the rotationally dominated flow and is expected to depend on both action and rotation. The results of this analysis can be found in table 2.

Figures 7–9 are organized in order of increasing rotational effect and are representative samples of all the data (for all the data plots see Dickinson 1980). We can see the transition region between 0.5 slope ($\Omega = 0$) and 1.0 slope move from 26 cm below the grid in figure 7 to 11.5 cm in figure 8. In figure 9, with the highest rotational effect, one cannot discern a 0.5-slope region. It is clear that rotation causes the change of slope.

From dimensional analysis, the transition between the two regions for the front velocity should occur at a distance proportional to $(K/\Omega)^{\frac{1}{2}}$. For comparison, we used the intercept of the 0.5-line taken from the corresponding case of zero rotation (figures 3–5), and the extension of the observed line of 1.0 slope. This intercept distance d_k , or 'knee' of the curve, scales well with the prediction

$$d_k (K_g/\Omega)^{-\frac{1}{2}} = D_k = \text{const},$$

where the average $\bar{D}_k = 1.87$, as we show in table 3. The plot of the observations as $d(K_g/\Omega)^{-\frac{1}{2}}$ versus Ωt in figure 10 yields a good collapse of the data, and shows that the front between disturbed fluid and undisturbed fluid propagates at the wave speed $c \sim (K\Omega)^{\frac{1}{2}}$ at sufficiently large distances from the grid. Figure 10 shows one randomly chosen run from each parameter set shown in table 3. The lines in figure 10 are eye-fitted. The continuous sections delineate the zones of 0.5 and 1.0 slope, while the dashed sections show the transition zone. Note that the average value of D_k (1.87) falls near the centre of this zone.

<i>f</i>	1.55			2.0			2.5		
	<i>n</i>	$K_{\Omega}^{\frac{1}{2}}$	r^2	<i>n</i>	$K_{\Omega}^{\frac{1}{2}}$	r^2	<i>n</i>	$K_{\Omega}^{\frac{1}{2}}$	r^2
0.21	0.48	3.77	0.89	0.53	3.9	0.94	0.47	5.23	0.96
	0.98	0.74	0.93	0.88	1.24	0.91	0.94	1.14	0.96
0.54	0.50	4.81	0.85	0.55	4.32	0.93	0.42	5.95	0.87
	0.83	1.69	0.84	0.88	1.75	0.89	0.90	1.65	0.90
1.08	0.58	4.31	0.95	0.62	4.14	0.90	0.55	5.18	0.95
	0.92	1.95	0.95	0.99	1.67	0.98	0.97	1.92	0.94

TABLE 2. Fitting the front propagation data to $d = K^{\frac{1}{2}} t^n$. These are the results of linear regression. The upper line for each rotation rate is the result for the data in the rotationally unaffected layer where $d \propto t^{\frac{1}{2}}$. The lower line is for the rotationally affected zone where $d \propto t$ approximately. r^2 is the coefficient of determination.

Ω	<i>f</i>	d_k	D_k
0.21	1.55	27.0	2.0
0.21	2.0	26.0	1.6
0.21	2.5	27.0	1.6
0.54	1.55	19.5	2.3
0.54	2.0	18.0	1.8
0.54	2.5	20.0	1.9
1.08	1.55	11.5	1.9
1.08	2.0	12.5	1.8
1.08	2.5	14.5	1.9

TABLE 3. Scaling the ‘knee’ of the entrainment curves to determine the value

$$D_k = \frac{d_k}{(K_g)^{\frac{1}{2}}/\Omega}$$

for each parameter set. The average for the above data $\bar{D}_k = 1.87$.

5. Depth of the turbulent layer in the steady case

We were able to identify a layer of fixed depth d_1 in the rotating experiments after enough time had elapsed for a steady state to be achieved. We did this by adding dye at the level of the grid, which then diffused in a homogeneous, cloud-like manner until the level d_1 was reached. Then, over a short distance (usually 2–3 cm), the appearance of the dye changed at lower levels to a more ‘organized’ pattern containing vertically oriented sheets resembling drapery or Taylor’s ‘ink walls’ (Taylor 1921; Long 1954). After several minutes, the ‘turbulent’ zone was completely dyed, while the zone below showed vertical clear zones where there was no ink. From the aluminium flakes, we know that the turbulent zone contains ordinary three-dimensional turbulence, while the lower zone is typified by rotationally dominated turbulence with large vertical coherence. This is similar to the lengthening of the correlation lengthscales parallel to the rotation axis measured by Ibbetson & Tritton (1975). Figure 11 shows the turbulence in the non-rotating case, and figure 12, for approximately the same frequency, shows the effect of rotation. In figure 12, we can clearly see the d_1 of about 10 cm thickness with the rotationally affected flow below.

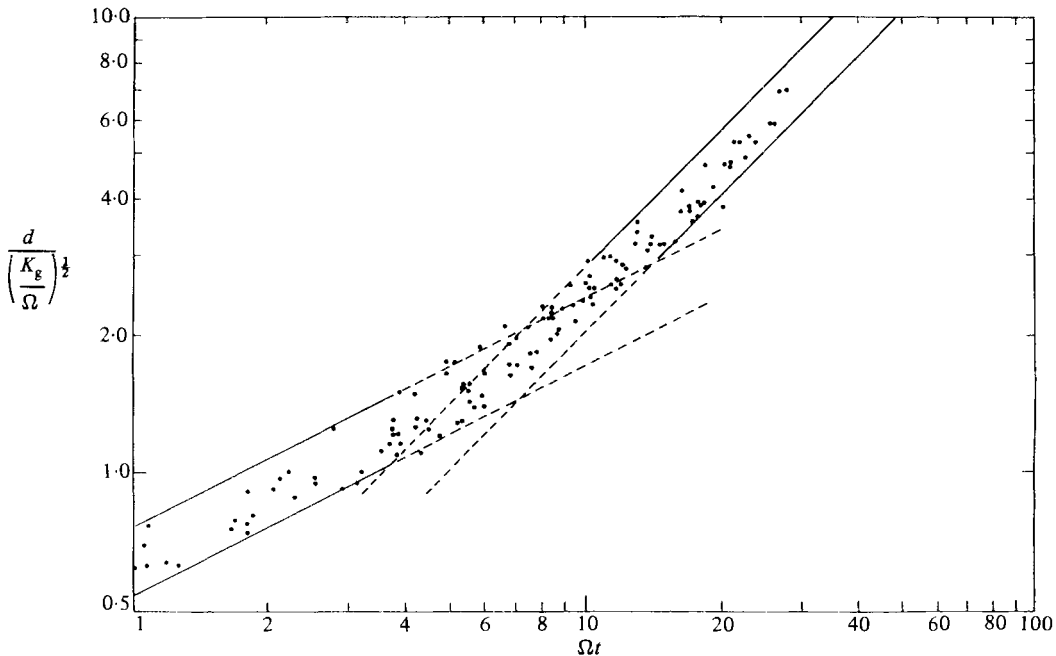


FIGURE 10. Plot of $d/(K_g/\Omega)^{\frac{1}{2}}$ versus Ωt from randomly selected runs showing collapse of data for various K and Ω .

The data from the dye technique is shown in figure 13; and that from a combination of dye and aluminium flakes in figure 14. Corresponding data are summarized in table 4. Figure 14 shows good agreement between the two methods, and figures 13 and 14 show good agreement with a proportionality of d_1 to $(K_g/\Omega)^{\frac{1}{2}}$. A regression analysis yielded $d_1 = (K_g/\Omega)^{0.48}$. Assuming, then, that with experimental error $d_1 = (K_g/\Omega)^{\frac{1}{2}}$, a linear regression for both the dye and aluminium flake methods yields the equation

$$d_1 = 1.65 \left(\frac{K_g}{\Omega} \right)^{\frac{1}{2}} + 1.15.$$

The constant $D_1 = 1.65$ is close to the constant $D_k = 1.87$ and indicates that D_1 and D_k are the same within experimental error. It appears from this that, for the steady case, there is no important effect of the bottom.

6. Motion of the turbulent front induced by an oscillating rod in rotating and non-rotating frames

The analogy between rotating and stratified fluids suggested to us, in the very early stages of this work, that the closest counterpart of the stratified-fluid experiments would be the propagation of a front *radially outward* from the axis of rotation of a rotating vessel where the turbulence was caused by a rod oscillating vertically along the axis. Although this did not become the central experiment of this paper, a few experiments were run using a rod of 0.64 cm diameter with O-rings 0.15 cm thick at 2.2 cm spacing to increase the turbulence. The stroke was 1.7 cm and the frequency 18.3 Hz, and these were held constant. We observed the average radius r of the turbulence as the cylindrical front propagated into the undisturbed fluid for both the rotating and non-rotating cases. These fronts, although harder to discern than

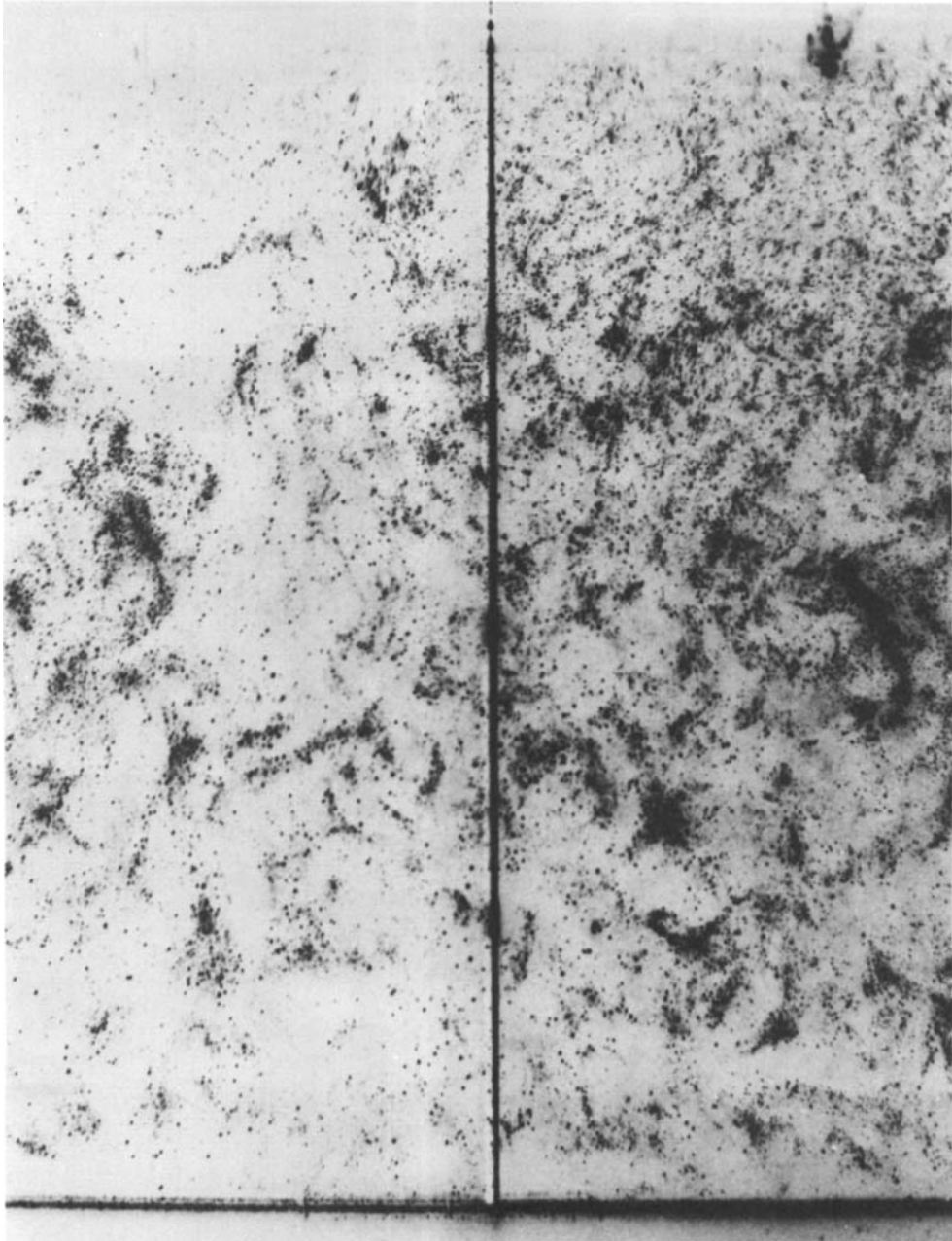


FIGURE 11. Photograph of oscillating-grid turbulence without rotation for $f = 2.0$ Hz.

those created by the oscillating grid, fit the $r = t^{\frac{1}{2}}$ curve reasonably well, as we see in figure 15. It is worthy of note that, especially in the non-rotating case, it was hard to obtain a cylinder of turbulence because the stirred fluid drifted off-axis as the experiment progressed. Increasing the rotation rate helped to stabilize the position of the stirred fluid. With rotation, the front would start at the rod and propagate out, eventually reaching a 'final' radius r_f as we see in figure 15. We found that r_f did not scale well on $(K_g/\Omega)^{\frac{1}{2}}$.

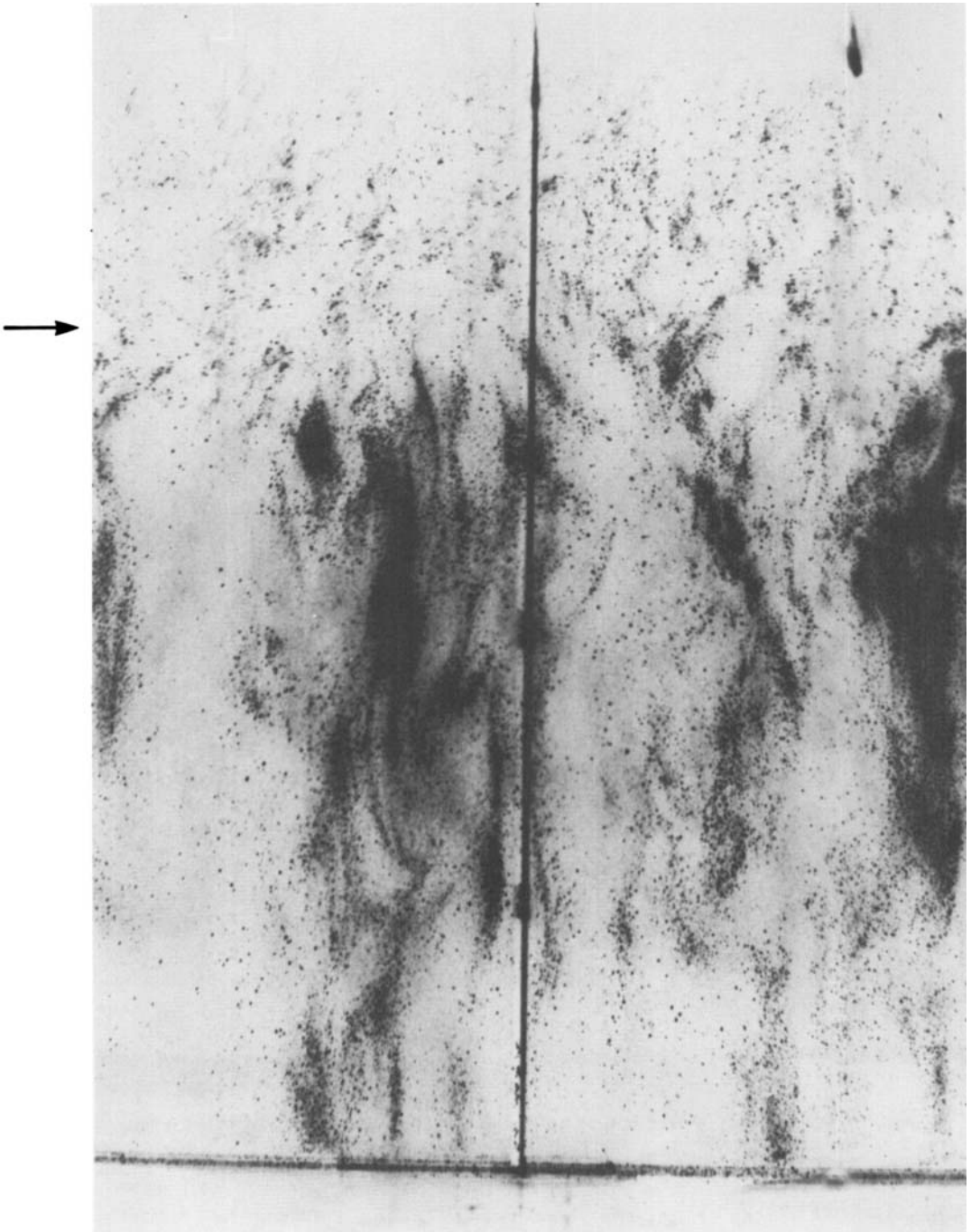


FIGURE 12. Photograph of oscillating-grid turbulence with rotation showing the layer d_1 above the arrows and the rotationally affected zone below; $f = 1.8$ Hz, $\Omega = 0.85$ rad/s.

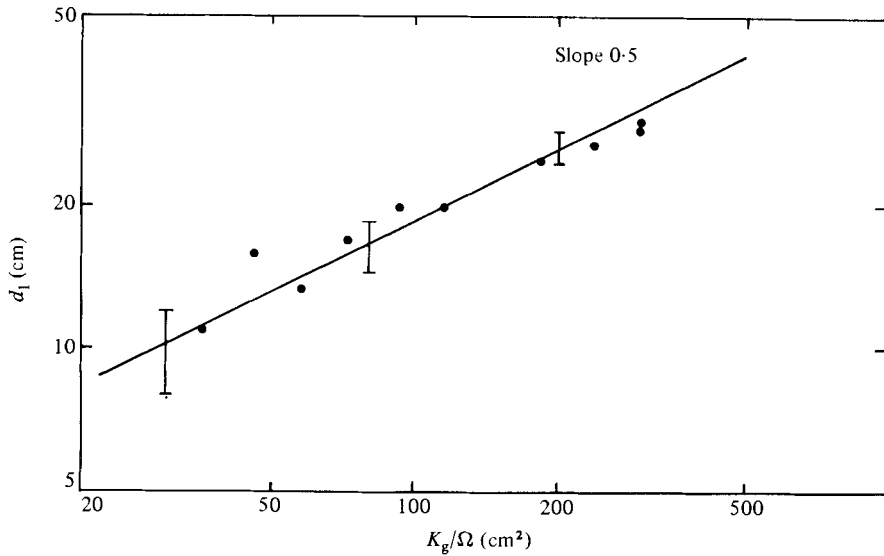


FIGURE 13. Plot of d_1 versus K_g/Ω using dye to identify the layer.

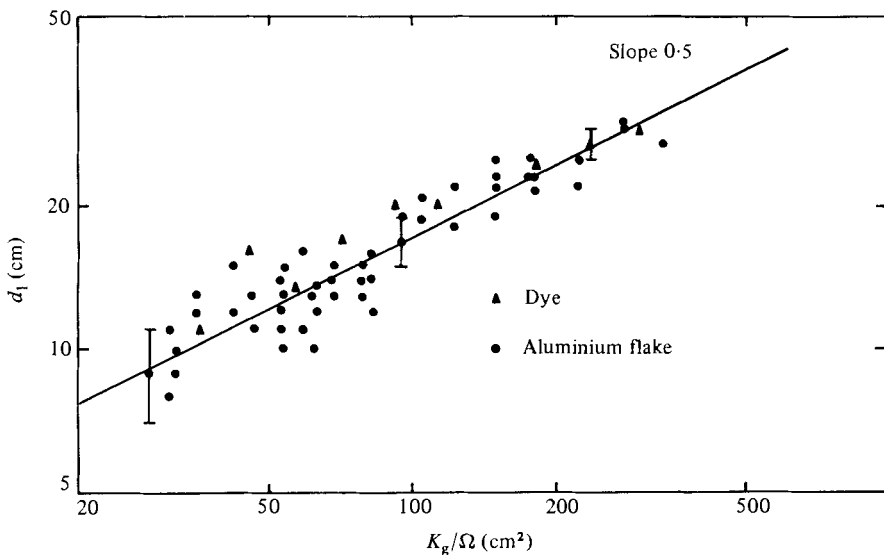


FIGURE 14. Plot of d_1 versus K_g/Ω using dye and aluminium flakes to identify the layer.

7. Discussions and conclusions

We have examined certain aspects of spatially decaying turbulence produced by an energy source on a plane. This turbulence appears to be as fundamental as the decaying turbulence behind a grid in a wind tunnel; and besides, it may occur frequently in natural circumstances; for example, below breaking surface waves in the ocean or, perhaps, in shear flow near a wall as the residual turbulence after 'bursts' and 'sweeps' and the 'sloshing' motion of the large eddies is subtracted out.

In the first experiment, turbulent layers created by an oscillating grid (which we believe to be similar to a planar turbulent energy source) are observed to increase

f (Hz)	Ω (rad/s)	d_1 (cm)	$\left(\frac{K}{\Omega}\right)^{\frac{1}{2}}$
Aluminium flakes			
1.2	0.20	19, 23	12.25
1.2	0.38	15, 13	8.90
1.2	0.55	13, 15	7.40
1.2	0.71	12, 15	6.50
1.2	0.85	13, 12	5.90
1.2	0.98	11, 8	5.50
1.2	1.08	9, 11	5.30
1.8	0.20	22, 25	15.0
1.8	0.38	23, 22	10.9
1.8	0.55	14, 14	9.0
1.8	0.71	12, 13	8.0
1.8	0.85	10, 14	7.3
1.8	0.98	13, 11	6.8
1.8	1.08	9, 10	6.4
2.3	0.20	30, 29	17.0
2.3	0.38	22, 25	12.3
2.3	0.55	21, 19	10.2
2.3	0.71	12, 16	9.0
2.3	0.85	14, 14	8.2
2.3	0.98	16, 11	7.7
2.3	1.08	11, 12	7.3
2.7	0.20	27	18.4
2.7	0.38	25, 23	13.3
2.7	0.55	22, 18	11.0
2.7	0.71	19, 17	9.8
2.7	0.85	15, 14	8.9
2.7	0.98	15, 13	8.3
2.7	1.08	13, 10	7.9
Dye			
2.0	1.08	16, 16	6.8
2.0	0.54	20	9.62
2.0	0.21	27	15.43
2.5	1.08	13.5	7.61
2.5	0.54	20.0	10.76
2.5	0.21	30.0	17.25
1.55	1.08	11	5.99
1.55	0.54	17	8.47
1.55	0.21	25	13.59
2.5	0.21	29	17.25

TABLE 4. Measured values of d_1 and the corresponding values of $(K_g/\Omega)^{\frac{1}{2}}$ used in the linear regression to find $D_1 = 1.65$

in thickness diffusively as the square root of time $t^{\frac{1}{2}}$. This confirms a theory by (Long 1978*a, b*) in which the constant of proportionality is not $\nu^{\frac{1}{2}}$ as in viscous diffusion, but $K^{\frac{1}{2}}$, where K is a constant of the dimensions and character of eddy viscosity and is called the action of the grid. Linear dependence of action on grid frequency is also indicated by the experiments, and is in accord with classical ideas that molecular viscosity is unimportant at large Reynolds numbers.

Grid turbulence in a stably stratified fluid has been studied for a long time, and the second experiment of this paper extends such experiments to a system of equal

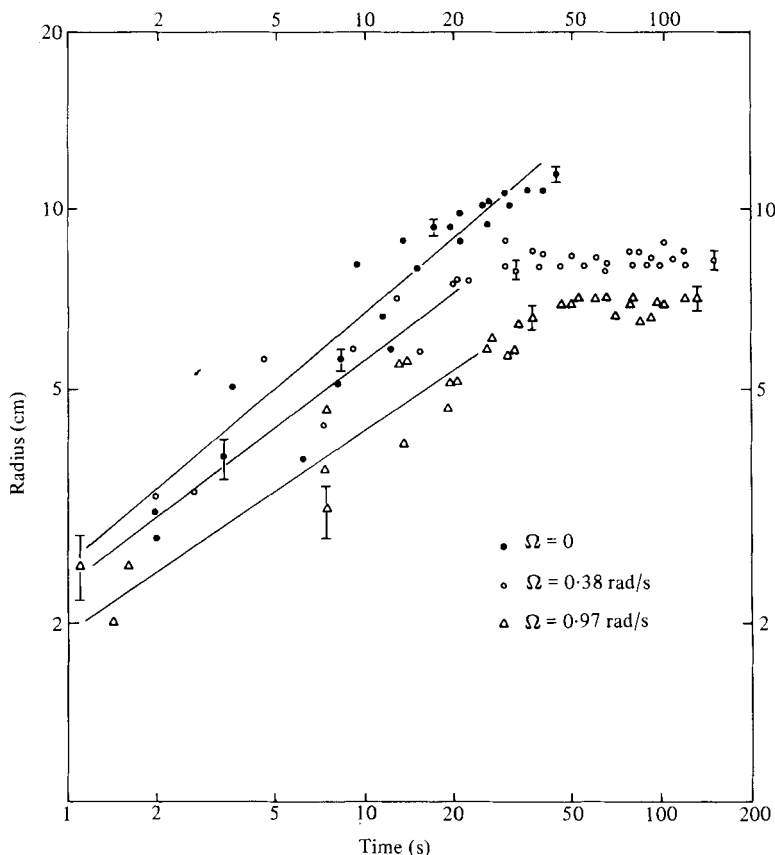


FIGURE 15. Plot of R versus t for oscillating rod.

geophysical importance, namely a fluid in solid-body rotation with angular velocity Ω . The axis of rotation is vertical, whereas the grid is horizontal and is oscillated vertically. After the oscillation starts, a turbulent layer in the vicinity of the grid grows with time and, as in the non-rotating case, its thickness d initially increases as $(Kt)^{\frac{1}{2}}$. The turbulence in this layer appears to be fully three-dimensional, horizontally homogeneous, and similar to that in the non-rotating case. For example, it rapidly and uniformly spreads dye over the whole layer. In the layer, the typical eddy size l should be proportional to the depth. Since K has the nature of eddy viscosity, it is proportional to σl , where σ is the r.m.s. velocity typical of the layer. Thus $K/d^2\Omega \sim \sigma/\Omega l$ has the form of a Rossby number. We would then anticipate that the layer would grow to a depth proportional to $(K/\Omega)^{\frac{1}{2}}$, where the Rossby number is of order unity, and then stop, albeit with disturbances of a wavelike character continuing to propagate away. This was observed, and the layer depth d_1 was determined by two independent techniques to be approximately

$$d_1 = 1.75 \left(\frac{K_g}{\Omega} \right)^{\frac{1}{2}}.$$

This depth is closely analogous to the depth of the Ekman layer caused by the motion over a plate of fluid in a rotating system (Plate 1971). Experiments by Caldwell, Van Atta & Helland (1972), Kreider (1973) and Howroyd & Slawson (1975) have determined that the Ekman depth d_e is proportional to u_τ/Ω , where u_τ is the friction

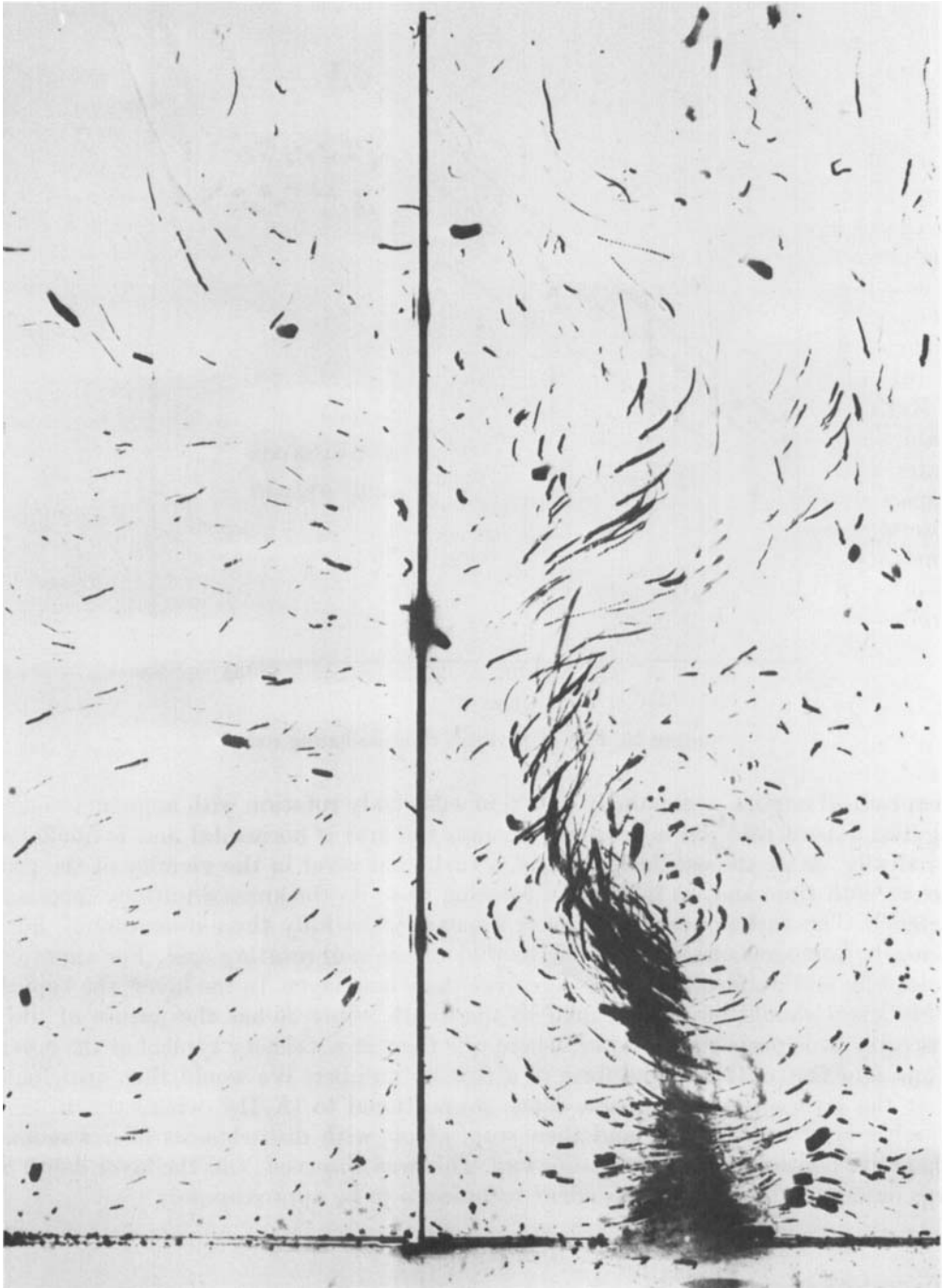


FIGURE 16. Photograph of polystyrene particles showing a 'McEwan-type' vortex of limited vertical extent; $f = 2.5$ Hz, $\Omega = 0.54$ rad/s.

velocity proportional to the velocity of the eddies in the layer. In accordance with classical ideas, the energy-containing eddies have vertical dimensions l of order d_e and so a characteristic eddy viscosity $\sigma l \sim u_\tau d_e$. Thus

$$d_e \sim \frac{u_\tau}{\Omega} \sim \frac{\sigma l}{\Omega d_e} \sim \frac{K}{\Omega d_e},$$

or
$$d_e \sim \left(\frac{K}{\Omega}\right)^{\frac{1}{2}},$$

establishing the analogy.

The experiments indicate that the front between the wavelike disturbances and the undisturbed fluid below propagate at an approximately constant speed $(K\Omega)^{\frac{1}{2}}$. This is proportional to the group velocity along the axis of rotation of waves of zero frequency and wavelength of the order of the depth of the three-dimensional turbulence; or, more appropriately, to the size of the eddies causing the wave disturbances. These appear to be columnar along the axis of rotation.

McEwan (1976) constructed a similar rotating-fluid experiment in a cylinder of water 23 cm deep with some 200 holes with 2 cm spacing in the bottom, through which water was pumped into and out of the container. The incoming jets therefore had a spacing of $M = 4$ cm and a variable maximum velocity at jet exit of w_j . McEwan observed the statistically steady state and directed attention to the vortices that appeared and drifted about with axes parallel to the axis of rotation. Among other observations, he reported that steady vortices were absent at values of the Rossby number

$$\frac{w_j}{\Omega h} > 1.15,$$

where h is the total depth of the fluid.

We have stated that we believe the columnar and wave like motions in the fluid below the turbulent layer are rotationally affected. This is the region where McEwan vortices could appear and indeed were occasionally observed in our experiments. Figure 16 shows a photograph of such a vortex (visualized by a one-second exposure of polystyrene particles) in a case where $d_1 = 18$ cm. We can see the vertical limit of the vortex. These vortices would be absent if the layer of three-dimensional turbulence filled the whole vessel; i.e. if $d_1 > h$. Using $d_1 = 1.75(K_g/X)^{\frac{1}{2}}$ we predict an absence of vortices at

$$\frac{K_g}{\Omega h^2} > 0.33. \quad (6)$$

If we take $w_j M = K_g$ and use $M/h = \frac{4}{23}$, McEwan's observed criterion for absence of vortices is

$$\frac{K_g}{\Omega h^2} > 0.20. \quad (7)$$

The fair agreement between (6) and (7) is encouraging in view of the rough estimate of K_g , and this relationship leads us to believe that we have offered a correct, partial explanation for the existence and non-existence of McEwan vortices.

We wish to acknowledge the support of the Office of Naval Research, Fluid Dynamics Division, under Contract N00014-76-C-0184 and by the National Science Foundation, Grants no. ATM-7907026 and OCE-76-18887.

REFERENCES

- BOUVARD, M. & DUMAS, H. 1967 Application de la méthode du fil chaud à la mesure de la turbulence dans l'eau. Deuxième parti. Exécution des mesures et résultats. *Houille Blanche* **22**, 723–734.
- BRETHEERTON, F. P. & TURNER, J. S. 1968 On the mixing of angular momentum in a stirred rotating fluid. *J. Fluid Mech.* **32**, 449–464.
- BRUSH, L. M. 1970 Artificial mixing of stratified fluids formed by salt and heat in a laboratory reservoir. *N.J. Water Resources Res. Inst. Res. Proj.* B-204.
- CALDWELL, D. R., VAN ATTA, C. W. & HELLAND, K. N. 1972 A laboratory study of the turbulent Ekman layer. *Geophys. Fluid Dyn.* **3**, 126–160.
- CRAPPER, P. F. & LINDEN, P. F. 1974 The structure of turbulent density interfaces. *J. Fluid Mech.* **65**, 45–63.
- CROMWELL, T. 1960 Pycnoclines created by mixing in an aquarium tank. *J. Marine Res.* **18**, 73–82.
- DICKINSON, S. C. 1980 Oscillating grid turbulence, including the effects of rotation. Ph.D. thesis, The Johns Hopkins University.
- DICKINSON, S. C. & LONG, R. R. 1978 Laboratory study of the growth of a turbulent layer of fluid. *Phys. Fluids* **21**, 1698–1701.
- FOLSE, R. F., COX, T. P. & SCHEXNAYDER, K. R. 1981 Measurements of the growth of a turbulently mixed layer in a linearly stratified fluid. *Phys. Fluids* **24**, 396–400.
- HOPFINGER, E. J. & TOLY, J. A. 1976 Spatially decaying turbulence and its relation to mixing across density interfaces. *J. Fluid Mech.* **78**, 155–175.
- HOWROYD, G. C. & SLAWSON, P. R. 1975 The characteristics of a laboratory produced turbulent Ekman layer. *Boundary-Layer Met.* **8**, 201–219.
- IBBETSON, A. & TRITTON, D. J. 1975 Experiments on turbulence in a rotating fluid. *J. Fluid Mech.* **68**, 639–672.
- KREIDER, J. F. 1973 A laboratory study of the turbulent Ekman layer. Ph.D. thesis, University of Colorado.
- KÜCHEMANN, D. 1965 Report on the I.U.T.A.M. symposium on concentrated vortex motions in fluids. *J. Fluid Mech.* **21**, 1–20.
- LINDEN, P. F. 1971 Salt fingers in the presence of grid-generated turbulence. *J. Fluid Mech.* **49**, 611–624.
- LINDEN, P. F. 1973 The interaction of a vortex ring with a sharp density interface: a model for turbulent entrainment. *J. Fluid Mech.* **60**, 467–480.
- LONG, R. R. 1954 Note on Taylor's 'Ink Walls' in a rotating fluid. *J. Met.* **11**, 247–249.
- LONG, R. R. 1978*a* Theory of turbulence in a homogeneous fluid induced by an oscillating grid. *Phys. Fluids* **21**, 1887–1888.
- LONG, R. R. 1978*b* The decay of turbulence. *The Johns Hopkins Univ. Tech. Rep.* No. 13 (Ser. C).
- MCDUGALL, T. J. 1979 Measurements of turbulence in a zero-mean-shear mixed layer. *J. Fluid Mech.* **94**, 409–431.
- MCEWAN, A. D. 1976 Angular momentum diffusion and the initiation of cyclones. *Nature* **260**, 126–128.
- PLATE, E. 1971 Aerodynamic characteristics of atmospheric boundary layers. *U.S. Atomic Energy Commission*.
- ROUSE, H. & DODU, J. 1955 Turbulent diffusion across a density discontinuity. *Houille Blanche* **10**, 405–410.
- STRITTMATTER, P. A., ILLINGWORTH, G. & FREEMAN, K. C. 1970 A note on the vorticity expulsion hypothesis. *J. Fluid Mech.* **43**, 539–544.
- TAYLOR, G. I. 1921 Experiments with rotating fluids. *Proc. R. Soc. Lond.* **100**, 114–121.
- THOMPSON, S. M. 1969 Turbulent interfaces generated by an oscillating grid in a stably stratified fluid. PhD Thesis, University of Cambridge.
- THOMPSON, S. M. & TURNER, J. S. 1975 Mixing across an interface due to turbulence generated by an oscillating grid. *J. Fluid Mech.* **67**, 349–368.
- TURNER, J. S. 1968 The influence of molecular diffusivity on turbulent entrainment across a density interface. *J. Fluid Mech.* **33**, 639–656.

- TURNER, J. S. 1973 *Buoyancy Effects in Fluids*. Cambridge University Press.
- TURNER, J. S. & KRAUS, E. B. 1967 A one-dimensional model of the seasonal thermocline. I. A laboratory experiment and its interpretation. *Tellus* **19**, 88–97.
- WOLANSKI, E. 1972 Turbulent entrainment across stable, density-stratified liquids and suspensions. PhD thesis, The Johns Hopkins University.
- WOLANSKI, E. J. & BRUSH, L. M. 1975 Turbulent entrainment across stable density step structures. *Tellus* **27**, 259–268.